

Characteristics and chemical reactivity of biogenic volatile organic compounds from dominant forest species in the Jing-Jin-Ji area, China

Ying Lin

Beijing Forestry University

Xiaoxiu Lun (✉ lunxiaoxiu@bjfu.edu.cn)

Beijing Forestry University

Wei Tang

CRAES: Chinese Research Academy of Environmental Sciences

Zhongzhi Zhang

Chinese Research Academy of Environmental Sciences

Xiaoxi Jing

Beijing Forestry University

Chong Fan

Beijing Forestry University

Research

Keywords: Biogenic volatile organic compounds (BVOCs), Isoprene, Monoterpenes, Jing-Jin-Ji area, Spatiotemporal characteristics, Chemical reactivity

Posted Date: January 27th, 2021

DOI: <https://doi.org/10.21203/rs.3.rs-97340/v2>

License: © ⓘ This work is licensed under a Creative Commons Attribution 4.0 International License.

[Read Full License](#)

Version of Record: A version of this preprint was published at Forest Ecosystems on August 1st, 2021. See the published version at <https://doi.org/10.1186/s40663-021-00322-y>.

**Characteristics and chemical reactivity of biogenic volatile organic compounds
from dominant forest species in the Jing-Jin-Ji area, China**

Ying Lin¹, Xiaoxiu Lun^{1*}, Wei Tang², Zhongzhi Zhang², Xiaoxi Jing¹, Chong Fan¹

¹College of Environmental Science and Engineering, Beijing Forestry University, 35
Tsinghua East Road, Beijing 100083, China

²Institute of Atmospheric Environment, Chinese Research Academy of Environmental
Sciences, Beijing 100012, China

*Corresponding author

Xiaoxiu Lun, #60, Beijing Forestry University, #35 Tsinghua East Road, Beijing 100083,
China. (E-mail: lunxiaoxiu@bjfu.edu.cn)

Abstract

Background: Biogenic volatile organic compounds (BVOCs) play an essential role in tropospheric atmospheric chemical reactions. There are few studies conducted on BVOCs emissions of dominant forest species in the Jing-Jin-Ji area. Based on the field survey, forest resources data and the measured standard emission factors, this paper applies the Guenther model developed in 1993 (G93) to estimate the emissions of BVOCs from several dominant forest species (*Platycladus orientalis*, *Quercus variabilis*, *Betula platyphylla*, *Populus tomentosa*, *Pinus tabulaeformis*, *Robinia pseudoacacia*, *Ulmus pumila*, *Salix babylonica* and *Larix gmelinii*) in the Jing-Jin-Ji area in 2017. Then the spatiotemporal emission characteristics and atmospheric chemical reactivity of these species were extensively evaluated.

Results: Results showed that the total annual BVOCs emissions were estimated to be 70.8 Gg C·a⁻¹, consisting of 40.5% (28.7 Gg C·a⁻¹) isoprene, 36.0% (25.5 Gg C·a⁻¹) monoterpenes and 23.4% (16.6 Gg C·a⁻¹) other VOCs. The emissions from *Platycladus orientalis*, *Quercus variabilis*, *Populus tomentosa* and *Pinus tabulaeformis* contributed 56.1%, 41.2%, 36.0% and 31.1%, respectively. In summer and winter, BVOCs emissions from the Jing-Jin-Ji area accounted for 61.9% and 1.8% of the annual total.

Up to 28.8% of emissions were detected from Chengde followed by Beijing with 24.9%, mainly distributed in the Taihang Mountains and the Yanshan Mountains. Additionally, the *Robinia pseudoacacia*, *Populus tomentosa*, *Quercus variabilis*, and *Pinus tabulaeformis* contributed mainly to BVOCs reaction activity.

Conclusions: Emissions peaked in summer (June, July, and August) and bottomed out in winter (December, January, and February). Chengde contributed the most, followed by Beijing. *Platycladus orientalis*, *Quercus variabilis*, *Populus tomentosa*, *Pinus tabulaeformis* and *Robinia pseudoacacia* represent the primary contributors to BVOCs emissions and atmospheric reactivity, hence the planting of these species should be reduced.

Keywords

Biogenic volatile organic compounds (BVOCs); Isoprene; Monoterpenes; Jing-Jin-Ji area; Spatiotemporal characteristics; Chemical reactivity

1. Background

Biogenic volatile organic compounds (BVOCs) are low boiling point compounds commonly synthesized by secondary metabolic pathways in plants. Many vascular plants can discharge BVOCs into the atmosphere (Loreto and Schnitzler, 2010). Forest is one of the primary sources that emit BVOCs, which occupies about 70% of the total BVOCs amounts from vegetation. It was estimated that the annual emissions of BVOCs in the world was about $10^6 \text{ Gg C} \cdot \text{a}^{-1}$ (Guenther et al., 2012), accounting for more than 90% of the total non-methane volatile organic compounds (NMVOCs) emissions on the ground and far exceeding the anthropogenic compounds (Guenther et al., 1995). Isoprene (the simplest 5-carbon isoprenoid, C_5H_8 , 2-methyl 1,3-butadiene) represents the highest emission component (Atkinson and Arey, 2003), with approximately 50% of the total annual global emissions of BVOCs around 412-601 $\text{Tg C} \cdot \text{a}^{-1}$ (Guenther et al. 2012). Monoterpenes are the 10-carbon isoprenoids that account for about 15% (32-157

Tg C·a⁻¹) of global BVOCs emissions (Guenther et al., 2012). Both isoprene and monoterpenes are synthesized by the MEP pathway (Loreto and Schnitzler, 2010). BVOCs are usually formed constitutively or after stress induction. Those components can improve plant tolerance to abiotic stressors such as high temperature, oxidative stress and biotic stressors (e.g. competing plants and microorganisms) (Loreto and Schnitzler, 2010; Filella et al., 2013).

BVOCs play an essential role in tropospheric atmospheric chemical reactions (Sartelet et al., 2012; Kulmala et al., 2013). BVOCs are main precursors to form tropospheric ozone and atmospheric aerosols, promoting the formation of secondary pollutants such as peroxyacetyl nitrate (PANs), secondary organic aerosols (SOA), particulate matter (PM), aldehydes and ketones (Claeys et al., 2004; Laothawornkitkul et al., 2009). In particular, the formation of ozone occurs when the isoprene is dissociated and react with NO_x (Fehsenfeld et al., 1992) while the formation medium of secondary organic aerosols (Claeys et al., 2004) is contributed by monoterpenes and sesquiterpenes via cloud condensation nuclei, hence affecting the local or global climate.

The Jing-Jin-Ji area that is locating on the North China Plain represents the core of north China and the most developed city cluster in China. With the rapid development of the economy and the acceleration of urbanization, the issue of air pollution requires immediate attention. The Jing-Jin-Ji area has been plagued by severe photochemical pollution and haze for many years (Tang et al., 2009; Han et al., 2013). It is known that

the accumulation of particulate matter, mostly fine particulate matter PM_{2.5} is the main factor that causes the haze (Hsu et al., 2017; Zhai et al., 2016; Li et al., 2013). Zhao et al. (2013) showed that the hourly average concentration of PM_{2.5} in Beijing reached 318 µg/m³ on hazy days. Several cities in Hebei province suffered more severe air pollution (Wang et al., 2012). Li et al. (2016) used PM_{2.5} monitoring data of 161 cities to analyze the PM_{2.5} pollution in mainland China. The results showed that the Jing-Jin-Ji and surrounding areas were heavily polluted and ranked at one of China's current four smoggy regions. Zhao et al. (2020) demonstrated that the average annual PM_{2.5} concentration in the Jing-Jin-Ji area decreased by 8.66 µg/m³ from 2014 to 2018, indicating the population that exposed to high PM_{2.5} concentration was decreasing. However, the average annual PM_{2.5} concentration value was still far from the national standard limit (35 µg/m³). Also, the ozone is another important pollutant that plagues the urban ambient air quality after PM_{2.5} (Meng et al., 2017). Chen et al. (2013) reported that the ozone mixing ratio in the Jing-Jin-Ji area was very high, thus causing strong photochemical reactions from May to September. Wang et al. (2017) pointed out that the ozone concentration had exceeded the standard by 100%-200% in the Jing-Jin-Ji area. During 2014-2018, the ozone concentration in the Jing-Jin-Ji area showed an upward trend with a positive average annual level of 4.90 µg/m³ as reported by Zhao et al. (2020). Some studies indicated that the contribution of BVOCs such as monoterpenes and sesquiterpenes to SOA formation was substantial (Steinbrecher et al., 2009; Aksoyoglu et al., 2011). Ghirardo et al. (2016) found that the contribution of BVOCs

released by vegetation to SOA generation in Beijing was increased by two-fold within 2005-2010. Carlo et al. (2004) reported that isoprene is highly reactive with hydroxyl radical ($\cdot\text{OH}$) than most anthropogenic volatile organic compounds (AVOCs). Geng et al. (2011) suggested that BVOCs can contribute to the surface ozone concentrations. The above literatures shown that the role of BVOCs in ozone formation cannot be ignored in the Jing-Jin-Ji area especially during summer (Ran et al., 2011; Xie et al., 2008), which would have led to severe impacts on human health, economic development, ecological environment, and climate change (Sicard et al., 2017). Considering the particular geographical location, diverse vegetation composition, and the enormous influence of BVOCs on ozone and secondary aerosols, it is crucial to clarify the BVOCs emitted from dominant forest species in the Jing-Jin-Ji area.

At present, estimates of BVOCs emissions from plants have been conducted through various studies using different methods including models, land cover and meteorological data. Different results of the Jing-Jin-Ji area were obtained from different models and input parameters at home and abroad (Kilnger et al., 2002; Song et al., 2012; Li et al., 2016). Most of the previous estimations were conducted by grouping the forest species into several plant functional types (PFT), using the global average emission rates and biomass density of each vegetation type. However, such estimations are unsatisfactory because the differences between plant species and regions are ignored (Xia and Xiao, 2019). Besides, most of the studies employed the recommended values of emission factors in the literature directly or select the measured values of adjacent

areas without the local measured primary data, hence the final results may not be representative (Song et al., 2012; Zhang et al., 2018). Different forest species or regions with different environments will cause different emission components and release rates of BVOCs (Owen et al., 2002). The difference between the forest species could be the primary factor determining the BVOCs emissions, and different geographical locations own disparate environmental conditions (temperature, PAR), which will also distinguish the emissions eventually. Therefore, the precise emission rates and fluxes of BVOCs from specific forest species in different regions should be obtained prior to evaluate the spatiotemporal effects and interactions of BVOCs on the atmospheric environment. Until present, there has been seldom evidence that supports the systematic comparison of the BVOCs measured emission rates of dominant forest species in the Jing-Jin-Ji area. According to the order of volume from high to low, we have selected *Platycladus orientalis*, *Quercus variabilis*, *Betula platyphylla*, *Populus tomentosa*, *Pinus tabuliformis*, *Robinia pseudoacacia*, *Ulmus pumila*, *Salix babylonica* and *Larix gmelinii* as the dominant forest species in the Jing-Jin-Ji area. Based on the field vegetation investigation and measured forest species emission rates, this paper applied Guenther model developed in 1993 (G93) (Guenther et al., 1993) to estimate the BVOCs emissions from dominant forest species in the Jing-Jin-Ji area, and analyze their spatiotemporal distribution characteristics and chemical reactivity, to establish a more localized emission inventory to eliminate its uncertainty further.

2. Materials and Methods

2.1 Site description

Jing-Jin-Ji area is located in the North China Plain (**Figure 1**), including Beijing, Tianjin, and Hebei ($36^{\circ} 05' - 42^{\circ} 40' \text{ N}$, $113^{\circ} 27' - 119^{\circ} 50' \text{ E}$), with a total area of about 21.72 ha. This area is surrounded by Bohai Sea in the east, Tai-hang Mountains in the West and Yanshan Mountains in the north, 735 km from north to south, and 576 km from east to west, with various terrains and warm temperate continental monsoon climate. The annual average temperature ranges from 0 to 13 °C with an average yearly precipitation of 300-800 mm. There are various vegetation types in this area including forest, shrub, grassland, and so on. The sampling sites were selected in the forest parks with abundant plant resources and the collection of the sample was performed on bright days.

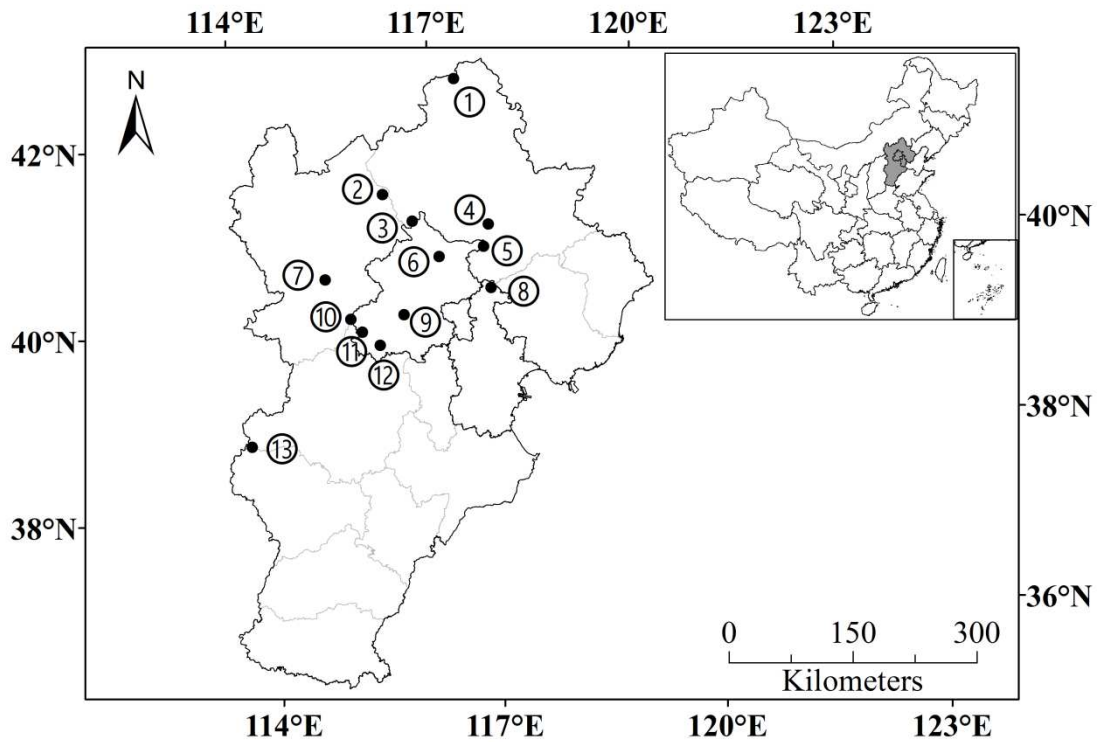


Figure 1. The site locations of the Jing-Jin-Ji area

The sampling sites (solid circles) identified as follows: ① Saihanba National Forest Park ② Heilongshan National Forest Park ③ Labagou Primeval Forest Park ④ Baicaowa National Forest Park ⑤ Wuling Mountain Scenic Spot ⑥ Yunmengshan National Forest Park ⑦ Huangyangshan Forest Park ⑧ Tianjin Jiulongshan National Forest Park ⑨ Xishan National Forest Park ⑩ Xiaolongmen National Forest Park ⑪ Baihuashan National Nature Reserve ⑫ Shangfangshan National Forest Park ⑬ Wuyuezhai Scenic Spot

2.2 Estimation model of BVOCs emission

Guenther series models are widely used to estimate BVOCs emissions. Guenther combined the latest experimental data to deduce the G93 algorithm in 1993 (Guenther et al., 1993). The model was used to normalized the emission rate of BVOCs under various environmental conditions, including $T=303$ K and $PAR=1000 \text{ mol}\cdot\text{m}^{-2}\text{s}^{-1}$ to match the estimation method of subdivision species selected in this paper. The BVOCs emitted by dominant forest species were classified as isoprene, monoterpene, and other VOCs (alcohols, aldehydes, ketones, organic acids, low carbon alkanes and alkenes) in this paper. According to the model of light and temperature effect proposed by G93, the BVOCs emissions classified by forest species were estimated respectively. Specific formulas are as follows:

$$\text{Isoprene: } I = I_S \times C_L \times C_{TI} \quad (1)$$

Where, I is the emission rate of isoprene (in C, $\mu\text{g}\cdot\text{g}^{-1}\cdot\text{h}^{-1}$) at a specific temperature T (K) and PAR ($\mu\text{mol}\cdot\text{m}^{-2}\cdot\text{s}^{-1}$), and I_S is the emission rate (standard emission rate) of isoprene (in C, $\mu\text{g}\cdot\text{g}^{-1}\cdot\text{h}^{-1}$) under standard condition ($T=303$ K, $\text{PAR}=1000$ $\mu\text{mol}\cdot\text{m}^{-2}\cdot\text{s}^{-1}$); C_L and C_{TI} are correction factors for light and temperature, respectively, that can be obtained by equations (2) and (3):

$$C_L = \alpha C_{L1} L / \sqrt{1 + \alpha^2 L^2} \quad (2)$$

Where, α (0.0027) and C_{L1} (1.066) are empirical constants, and L is PAR.

$$C_{TI} = \frac{\exp[C_{T1}(T - T_s)/RT_s T]}{1 + \exp[C_{T2}(T - T_M)/RT_s T]} \quad (3)$$

Where, R is a gas constant (8.314 $\text{J}\cdot\text{K}^{-1}\cdot\text{mol}^{-1}$); T_s is the leaf temperature of the standard state (303 K). C_{T1} (95000 $\text{J}\cdot\text{mol}^{-1}$), C_{T2} (230000 $\text{J}\cdot\text{mol}^{-1}$) and T_M (314 K) are empirical constants.

The monoterpenes and other VOCs emission rates in algorithm G93 can be calculated using equation (4) and (5):

$$M = M_{TS} C_{TM} \quad (4)$$

$$C_{TM} = \exp[\beta (T - T_s)] \quad (5)$$

Where M is the emission rate of monoterpene and other VOCs (in C, $\mu\text{g}\cdot\text{g}^{-1}\cdot\text{h}^{-1}$) at a certain temperature T (K); M_{TS} is the emission rate (basic emission rate) of monoterpene

and other VOCs (in C, $\mu\text{g}\cdot\text{g}^{-1}\cdot\text{h}^{-1}$) under standard condition ($T_s=303\text{ K}$); C_{TM} is correction factor for temperature of monoterpenes and other VOCs; β (0.09 K^{-1}) is empirical constant.

Experimental results showed that the emission rate of isoprene is mainly controlled by leaf temperature and PAR. However, the main factor affecting monoterpenes and other VOCs emission by plants is temperature. Therefore, the emission estimation method of isoprene is:

$$E_{ISOP}=I_S\times B\times C_{TI}\times C_L \quad (6)$$

The emission estimation method of monoterpenes and other VOCs is:

$$E_{MONO}, E_{OVOC}=M_{TS}\times B\times C_{TM} \quad (7)$$

Where, E_{ISOP} is the emission of isoprene (in C, $\mu\text{g}\cdot\text{h}^{-1}$); E_{MONO} and E_{OVOC} are the emissions of monoterpenes and other VOCs (in C, $\mu\text{g}\cdot\text{h}^{-1}$), respectively; and B is the leaf biomass (dry weight, g) of each species. The required meteorological data (temperature and PAR of every month in the Jing-Jin-Ji area in 2017) can be retrieved from MODIS satellite product data published on the NASA website (<https://modis.ornl.gov/data.html>).

2.3 Determination of model parameters

2.3.1 Emission rates

BVOCs were collected using a dynamic headspace method. The sampling system

consists of a transparent Teflon film sampling bag (10 L), an atmospheric sampler (LaoDong QC-1S, Beijing Municipal Institute of Labor Protection, China), two drying towers (filled with activated carbon particles that have been pre-dried for more than 5 h and allochroic silica gel), an ozone removal column (Cleanert KI: 1.4 g/2.5 mL, Agela Technologies, China) and an adsorption tube (tube type: stainless steel tube, Camsco company, USA, filled with Carbograph 2 (60/80), Carbograph 1 (40/60) and Carbosieve SIII (60/80) adsorbents). All parts are connected with polytetrafluoroethylene (PTFE) tubes (**Figure 2**). Before sampling, the adsorption tubes were purged and activated at 270 °C for 2 h under high-purity N₂ (purity: 99.99%), then stored under cold storage at 4 °C. The selected branches of forest species with healthy foliage were enclosed in the sampling bag, and the BVOCs were sampled at a flow rate of 1.5 L/min. The temperature, relative humidity and photosynthetic active radiation were recorded with a hand-held meteorological instrument at the same time. **Table 1** shows the average values of these parameters recorded during the sampling. After collection, the adsorption tube was stored in the refrigerator at 4 °C and analyzed within one week.

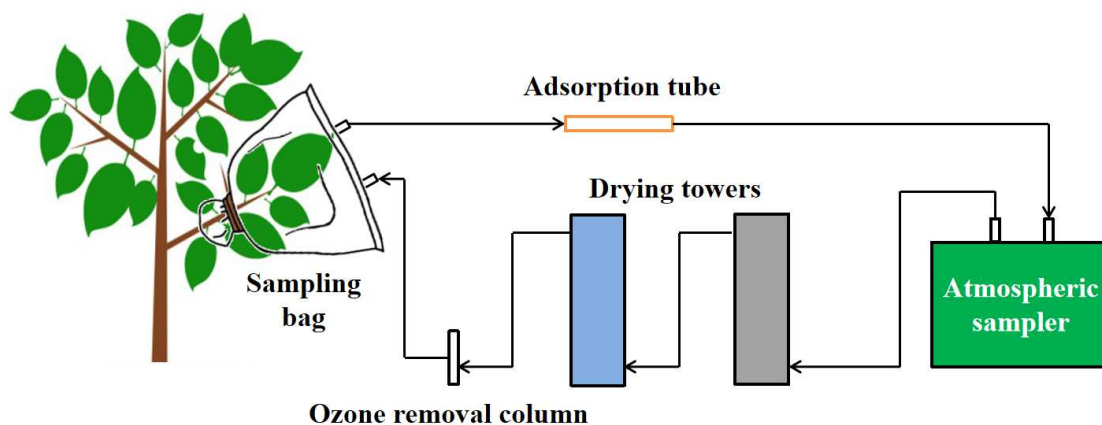


Figure 2. Flow chart of dynamic headspace sampling

BVOCs were adsorbed on PE TurboMatrix (650ATD-Clarus600) and analyzed by thermal desorption gas chromatography-mass spectrometry (TCT-GC-MS, Agilent 6890, USA). Most of the organics in the adsorption tube were released after 5 min in a thermal resolver at 260 °C, and then the substances were adsorbed into the cold trap (-25 °C). The substances condensed in the cold trap were quickly heated from 260 °C to 300 °C at a heating rate of 40 °C/s, followed by transferring to the chromatograph for separation and analysis. The mass spectrometer adopts electron bombardment ionization mode with an energy of 70 eV and a scanning atomic mass range of 30-500 amu. The compounds were retrieved from the database of National Institute of Standards and Technology (NIST) based on their retention times and specific charge and quantified using the standard external method. The following sources of standard gas were used: Photochemical Assessment Monitoring Stations (PAMS) (Spectra/Linde: 57), n-hexane (12.3 ppmV), isoprene (12.7 ppmV), α -pinene (10.3 ppmV), β -pinene (10.8 ppmV), α -phellandrene (8.45 ppmV), 3-carene (10.6 ppmV), myrcene (8.19 ppmV), α -terpinene

(7.12 ppmV), limonene (10.1 ppmV), γ -terpinene (7.81 ppmV), and ocimene (7.68 ppmV). The different volume of these standard gases were quantitatively diluted into Summa canisters and then collected into adsorption tubes for further analysis.

The emission rates of dominant forest species in the Jing-Jin-Ji area were respectively calculated according to the following equation:

$$ER = \frac{m}{t \times M} \quad (8)$$

Where, ER is the emission rate of each forest species (in C, $\mu\text{g}\cdot\text{g}^{-1}\cdot\text{h}^{-1}$); m is the quality of BVOCs in adsorption tube (in C, μg); t is the sampling time (h); M is the leaf biomass of forest species (dry weight, g).

The standard emission factors of each forest species corrected by the light and temperature model were detailed in elsewhere (Fan, 2019).

Table 1. Sampling dates and averaged environmental conditions during the samplings in 2018

Sampling Date	Binomial name	Region	¹ PAR ($\mu\text{mol}/\text{m}^2\text{s}$)	² T ($^{\circ}\text{C}$)	³ RH (%)
08/23-08/24	<i>Salix babylonica</i>	②/⑦/⑨	938	32.5	23.7
08/29-08/31	<i>Pinus tabuliformis</i>	①/⑤/⑨/⑩	1963	33.1	23.9
08/29-08/31	<i>Populus tomentosa</i>	①/④/⑤/⑦/⑧	1369	34.0	27.2
07/29-07/31	<i>Platycladus orientalis</i>	④/⑤/⑦/⑧/⑨	1606	34.2	27.4
08/29-08/30	<i>Robinia pseudoacacia</i>	⑤/⑦/⑬	1206	32.8	23.2
06/20-06/21	<i>Ulmus pumila</i>	②/④/⑦	1537	37.1	23.6
06/05-06/07	<i>Larix gmelinii</i>	①/④/⑤/⑥/⑩	1629	29.1	19.9

07/01-07/02	<i>Quercus variabilis</i>	⑧/⑨/⑫	1059	34.5	22.6
07/27-07/28	<i>Betula platyphylla</i>	①/③/⑩/⑫/⑬	875	31.0	24.3

① - ⑬ : The specific name of sampling place is shown in the note of Figure 1; ¹PAR: Photosynthetically active radiation; ²T: Temperature; ³RH: Relative humidity.

2.3.2 Leaf biomass calculation

The leaf biomass data in Jing-Jin-Ji area were obtained using the method of volume and yield conversion. The statistical method of subdividing species enables them to correspond to more appropriate emission factors and biomass, by considering the difference of the same species in different regions. Based on the volumes obtained from the national forest resource inventory, the leaf biomass of the dominant forest species can be calculated as follows:

$$B = \frac{V \times D_T}{P_T} \times P_L \quad (9)$$

Where B is leaf biomass of forest species (dry weight, g); V is tree volume; D_T is the basic density of tree trunk (the ratio of absolute dry wood mass to raw wood volume); P_T and P_L are the proportion of stem and leaf in the total biomass of tree layer respectively. The data of P_T , P_L and D_T were retrieved from literature (Wang et al., 2001). In this study, the proportion of trunk density, leaf and stem biomass to the total biomass of dominant forest species in the Jing-Jin-Ji area were presented in **Table A.1**. Tree volumes data were mainly based on national forest resources survey data, checked and supplemented by forestry network and field survey.

2.4 Methods of chemical activity evaluation

Different BVOCs components have different chemical compositions and physical properties, thus the atmospheric chemical reaction capacity is different (Goldan et al., 2004). Studying the chemical reactivity of different BVOCs and their ability to generate ozone can provide a reference for the control measures of BVOCs. This study adopted two methods, the maximum incremental reactivity (MIR) method and the $\cdot\text{OH}$ reaction rate (L^{OH}) method, to comprehensively analyze the chemical activity of the BVOCs components of dominant forest species in the Jing-Jin-Ji area.

Ozone formation potential (OFP) can be used to evaluate the potential release of BVOCs into the atmosphere under optimal reaction conditions for ozone generation and measure the reactivity of different BVOCs components (Carter, 1991). The calculation of OFP is shown in equation (10):

$$OFP_i = \text{MIR}_i \times C_i \quad (10)$$

Where OFP_i is the ozone generation potential of each component ($\mu\text{g}/\text{m}^3$); MIR_i is the maximum incremental response factor of each component (gO_3/gVOCs) (Carter, 2008); C_i is the mass concentration of each component ($\mu\text{g}/\text{m}^3$).

The chemical reaction of the troposphere during the daytime is mainly OH radicals ($\cdot\text{OH}$). The volatile organic compounds will first react with $\cdot\text{OH}$, and then react with O_2 and NO_x under light conditions to generate new free radicals to initiate a chain reaction. The first reaction is a key step that determines the rate of atmospheric photochemical

reaction chain, so the consumption rate of $\cdot\text{OH}$ can be used to evaluate the photochemical activity of BVOCs. The calculation is shown in equation (11):

$$L_i^{OH} = K_i^{OH} \times [BVOCs]_i \quad (11)$$

Where L_i^{OH} is the consumption rate of each component to atmospheric $\cdot\text{OH}$ (s^{-1}); K_i^{OH} is the reaction rate constant between each component and atmospheric $\cdot\text{OH}$ ($\text{cm}^3 \cdot \text{molecule}^{-1} \cdot \text{s}^{-1}$) (<https://kinetics.nist.gov/kinetics/index.jsp>); $[BVOCs]_i$ is the atmospheric molecular concentration of every component ($\text{molecule} \cdot \text{cm}^{-3}$).

3. Results and discussion

3.1 Emission budgets and compositions of BVOCs

BVOCs emitted from dominant forest species were divided into isoprene, monoterpenes, and other VOCs (OVOCs) (**Table 2**). The total annual emission of BVOCs from dominant forest species in the Jing-Jin-Ji area was estimated to be 70.8 $\text{Gg C} \cdot \text{a}^{-1}$, including 40.5% (28.7 $\text{Gg C} \cdot \text{a}^{-1}$) isoprene, 36.0% (25.5 $\text{Gg C} \cdot \text{a}^{-1}$) monoterpenes and 23.4% (16.6 $\text{Gg C} \cdot \text{a}^{-1}$) of other VOCs, respectively.

Monoterpenes comprises of α -pinene, β -pinene, β -myrcene, limonene, 3-carene and so on. Different forest species can produce various components of BVOCs. **Figure 3** shows each component and proportion of BVOCs emitted by nine dominant forest species in the Jing-Jin-Ji area. Isoprene was emitted as the main component from broadleaf trees such as *Betula platyphylla*, *Quercus variabilis*, and *Salix babylonica*. Aside from isoprene, some of the broadleaf trees (i.e. *Populus tomentosa*, *Robinia*

pseudoacacia, *Ulmus pumila*) and most coniferous trees like *Platycladus orientalis*, *Pinus tabuliformis*, and *Larix gmelinii* will release monoterpenes such as α -pinene, β -pinene, β -myrcene and limonene. As shown in **Figure A.1**, isoprene emission was mainly detected from *Quercus variabilis* and *Populus tomentosa* that recording at 41.2% and 31.1%, respectively. On the other hand, *Platycladus orientalis* and *Pinus tabuliformis* are the significant emitters of monoterpenes, providing 56.1% and 36.0%, respectively. Therefore, it was revealed that these four forest species are the main contributors to BVOCs emissions in the Jing-Jin-Ji area: 19.3 Gg C·a⁻¹ (27.2%) from *Platycladus orientalis*, 14.0 Gg C·a⁻¹ (19.8%) from *Quercus variabilis*, 13.4 Gg C·a⁻¹ (18.9%) from *Populus tomentosa* and 12.2 Gg C·a⁻¹ (17.2%) from of *Pinus tabuliformis* (**Table 2**).

Table 2. The annual emissions of BVOCs from dominant forest species in the Jing-Jin-Ji area (10⁶ g C·a⁻¹)

Forest species	Isoprene	α -pinene	β -pinene	β -myrcene	limonene	3-carene	¹ OVOCs	² TVOCs	Proportion
<i>Platycladus orientalis</i>	70.0	7591.2	318.2	1185.1	765.1	4446.0	4885.1	19260.6	27.2%
<i>Robinia pseudoacacia</i>	3375.0	209.7	150.4	57.4	90.5	32.5	1191.4	5107.0	7.2%
<i>Betula platyphylla</i>	2131.1	14.9	0.0	0.0	0.0	0.0	2232.4	4378.3	6.2%
<i>Quercus variabilis</i>	11818.3	0.0	0.0	0.0	0.0	0.0	2184.3	14002.6	19.8%

<i>Salix babylonica</i>	1637.2	0.0	0.0	0.0	0.0	0.0	190.7	1827.9	2.6%
<i>Populus tomentosa</i>	8934.9	464.7	48.4	279.3	255.2	2.7	3383.8	13368.9	18.9%
<i>Pinus tabuliformis</i>	707.7	3254.4	22.1	4041.9	1854.7	11.0	2263.0	12154.8	17.2%
<i>Ulmus pumila</i>	28.1	17.9	0.0	20.2	0.0	0.0	193.3	259.6	0.4%
<i>Larix gmelinii</i>	0.1	276.3	114.5	0.0	0.0	0.0	79.8	470.7	0.7%
Total	28702.3	11829.1	653.5	5583.9	2965.5	4492.2	16603.7	70830.2	100.0%
Proportion	40.5%	16.7%	0.9%	7.9%	4.2%	6.3%	23.4%	100.0%	-

¹OVOCs: other VOCs; ²TVOCs: total VOCs.

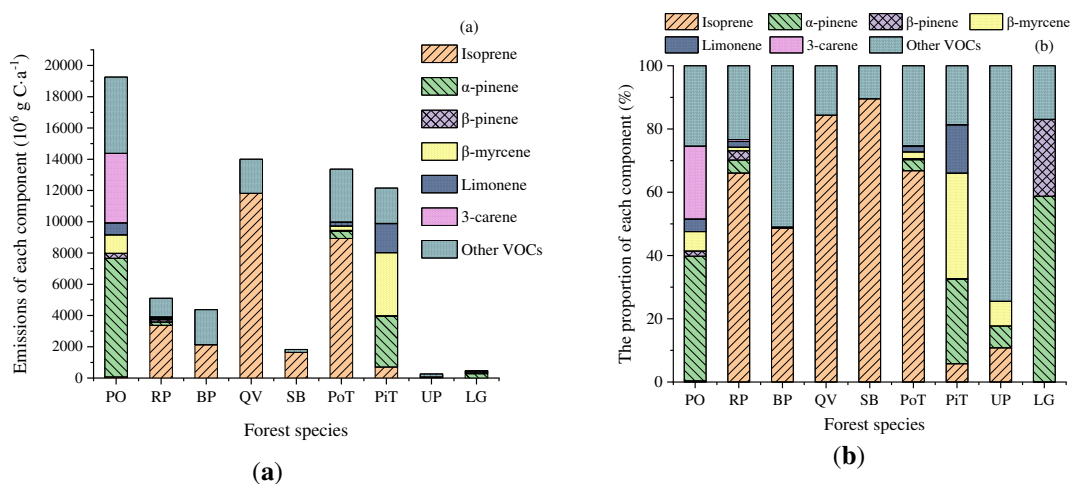


Figure 3. The BVOCs emissions ($10^6 \text{ g C}\cdot\text{a}^{-1}$) (a) and proportion of each component (%) (b) from dominant forest species in the Jing-Jin-Ji area

(BP: *Betula platyphylla*; QV: *Quercus variabilis*; UP: *Ulmus pumila*; PoT: *Populus tomentosa*; RP: *Robinia pseudoacacia*; PO: *Platyclusus orientalis*; PiT: *Pinus tabuliformis*; SB: *Salix babylonica*; LG: *Larix gmelinii*)

3.2 Monthly and Seasonal variations

As shown in equation (6) and (7), by multiplying the standardized emission factors, leaf biomass, parameters about meteorological data in 2017, and then accumulating them, the monthly BVOCs emissions were obtained. **Table A.2** and **Figure 4** indicate that the BVOCs emissions and compositions in the Jing-Jin-Ji area demonstrate significant variations, both monthly and seasonal. A distinct unimodal change with the month for the emissions of BVOCs was observed.

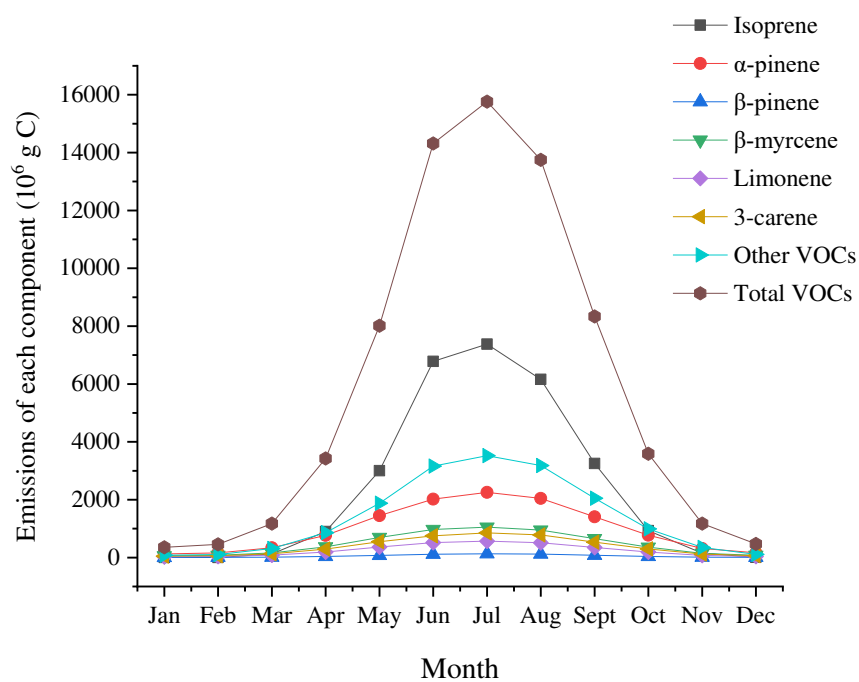


Figure 4. The monthly BVOCs emissions from dominant forest species in the Jing-Jin-Ji area (10^6 g C)

The total BVOCs emissions was peaked in July with a total amount of $15.8 \text{ Gg C}\cdot\text{a}^{-1}$, while recorded a minimum value in January of $0.4 \text{ Gg C}\cdot\text{a}^{-1}$ with two orders of magnitude difference. In January, the emission of isoprene from vegetation hit the lowest point at $1.9 \times 10^6 \text{ g C}\cdot\text{a}^{-1}$ due to low temperature, less sunlight, and the limited leaves of biomass. In contrast, the emission of isoprene achieved the highest point at $7.4 \text{ Gg C}\cdot\text{a}^{-1}$ in July when the air temperature was high, presence of strong sunlight, and abundant leaves of biomass. Nevertheless, the emission of isoprene fluctuated in other months between the maximum and minimum values obtained. The same trend was obtained from the emission of monoterpenes and other VOCs in which the highest emissions were recorded in July while the lowest emissions were detected in January.

Overall, the total BVOCs emissions were peaked in summer (June, July, and August) and bottomed out in winter (December, January and February). In spring, the BVOCs emissions showed an upward trend in which the isoprene was increased the most. Despite the emissions of both monoterpenes and other VOCs also increased, the values recorded were comparatively lower than the isoprene that could be due to the more significant influence of sunlight and temperature on isoprene. Under these conditions in spring, the vegetation is still in the growing stage where the leaves are immature and the

enzyme activity is still regular. Therefore, the emissions of BVOCs in spring only accounted for 17.8% in the whole year. Comparatively, the average daily temperature and sunshine time are significantly increased in summer than that in spring. Under these conditions, the vegetation leaves reached the mature stage and grown with maximum leaf area; consequently the highest enzyme activity was achieved. As a result, high emissions of BVOCs were observed in summer with the emissions of 43.8 Gg C·a⁻¹ that accounting for 61.9% of the total annual emissions. In autumn, the temperature difference was noticeable. The leaves were transformed from the mature leaves to the decaying leaves. Therefore, the emissions of BVOCs showed a decreasing trend in September, followed by a sharp decrease in October, and finally maintain in November. The total emissions of BVOCs recorded in autumn at only 18.5%. Due to low temperatures and limited solar irradiation in winter, the emissions of BVOCs reached the lowest value of the year at only 1.8%.

3.3 Spatial distribution

The BVOCs emissions of dominant forest species in 13 cities (Beijing, Tianjin, Baoding, Cangzhou, Chengde, Handan, Hengshui, Langfang, Qinhuangdao, Shijiazhuang, Tangshan, Xingtai, Zhangjiakou) throughout 2017 were calculated to study the spatial distribution of BVOCs emissions in the Jing-Jin-Ji area. As is shown in **Table A.3** and **Figure 5**, the BVOCs emission fluxes and compositions in the Jing-Jin-Ji area demonstrate an apparent spatial distribution. Given that Chengde and Beijing have high coverage of vegetation, and the presence of dominant species (*Betula platyphylla*,

Quercus variabilis, *Populus tomentosa* and *Pinus tabulaeformis*) in Wuling Mountain Reserve and Saihanba Forest Farm in Chengde showed higher BVOCs emission rates. Therefore, Chengde contributed the highest BVOCs emissions of dominant forest species in the Jing-Jin-Ji area with 20.4 Gg C·a⁻¹ (28.8%), followed by Beijing with a total discharge of 17.6 Gg C·a⁻¹ (24.9%). The remaining proportion of BVOCs emissions was detected from Baoding, Tangshan, Hengshui and Zhangjiakou. Furthermore, the detected BVOCs emissions of Cangzhou (0.4 Gg C·a⁻¹, 0.6%) and Langfang (0.5 Gg C·a⁻¹, 0.8%) were less than the others due to their smaller city area and lower vegetation coverage. In terms of compositions, as is shown in **Figure A.2**, Chengde presents the largest isoprene emission with 26.8% (7.7 Gg C·a⁻¹) of the total isoprene emissions released by dominant forest species in the Jing-Jin-Ji area. This could probably due to the extensive vegetation coverage of deciduous trees with high isoprene emissions such as *Quercus variabilis*. Besides from Chengde, Beijing also shows high emissions of monoterpenes (9.4 Gg C·a⁻¹) that accounting for 36.9% of the total monoterpenes emissions. This could be attributed to α -pinene and β -myrcene from coniferous such as *Platycladus orientalis* and *Pinus tabuliformis*, which could also explain the highest emissions detected for Chengde in spring, summer, and autumn, but lower than Beijing particularly in winter. Chengde possesses the most substantial difference in emissions in winter and summer because the dominant forest species here are mostly deciduous trees. The low temperature and less sunshine in winter would have caused the leaf biomass of deciduous trees to emit lower BVOCs; thus the emission was

reduced significantly (**Figure 6**). In general, the distribution of BVOCs emission fluxes is highly consistent with the distribution of vegetation.

Overall, the BVOCs emissions estimated in this study are much lower than those estimated by Klinger et al. (2002) (**Table 3**). It is due to the difference in the scope of the study objects, this study focused on specific dominant forest species while Klinger's research looked at all species in this area, including grasslands, shrublands, forests, and peatlands.

Table 3. Comparison of estimated BVOCs emissions in different provinces

Province	Emissions (10^9 g C·a ⁻¹)			References
	Isoprene	Monoterpenes	¹ OVOCs	
Beijing	13.9	7.8	26.3	Klinger et al. (2002)
Beijing	4.3	9.4	4.0	This study
Tianjin	2.6	1.4	22.2	Klinger et al. (2002)
Tianjin	3.2	0.8	0.4	This study
Hebei	99.2	50.9	321.0	Klinger et al. (2002)
Hebei	21.3	15.3	12.3	This study

¹OVOCs: other VOCs.

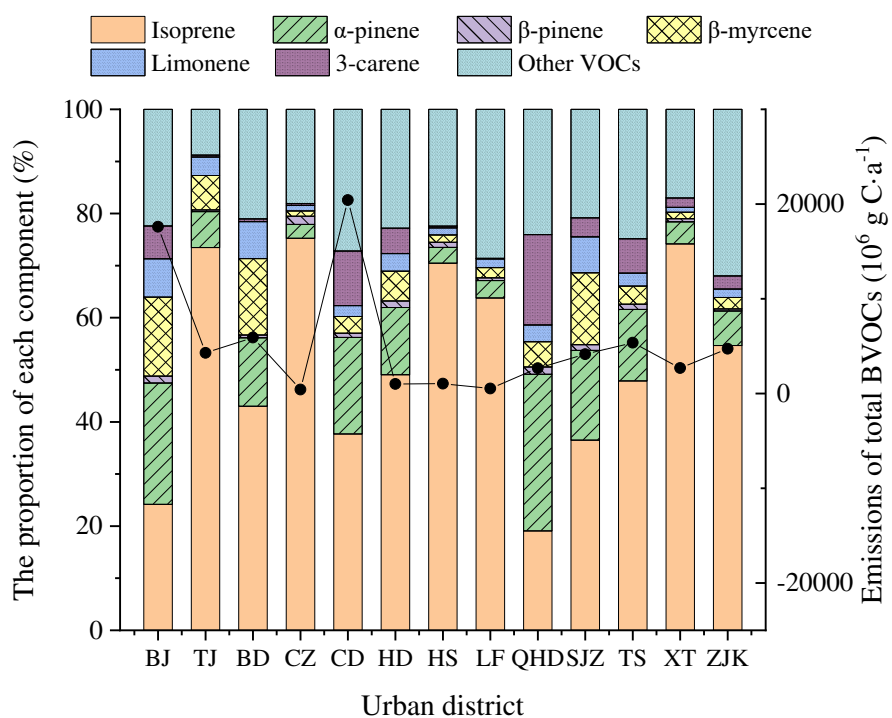


Figure 5. The BVOCs emissions ($10^6 \text{ g C}\cdot\text{a}^{-1}$) (a) and proportion of each component (%) (b) in each city in the Jing-Jin-Ji area

(BJ: Beijing; TJ: Tianjin; BD: Baoding; CZ: Cangzhou; CD: Chengde; HD: Handan; HS:

Hengshui; LF: Langfang; QHD: Qinhuangdao; SJZ: Shijiazhuang; TS: Tangshan; XT: Xingtai; ZJK:

Zhangjiakou)

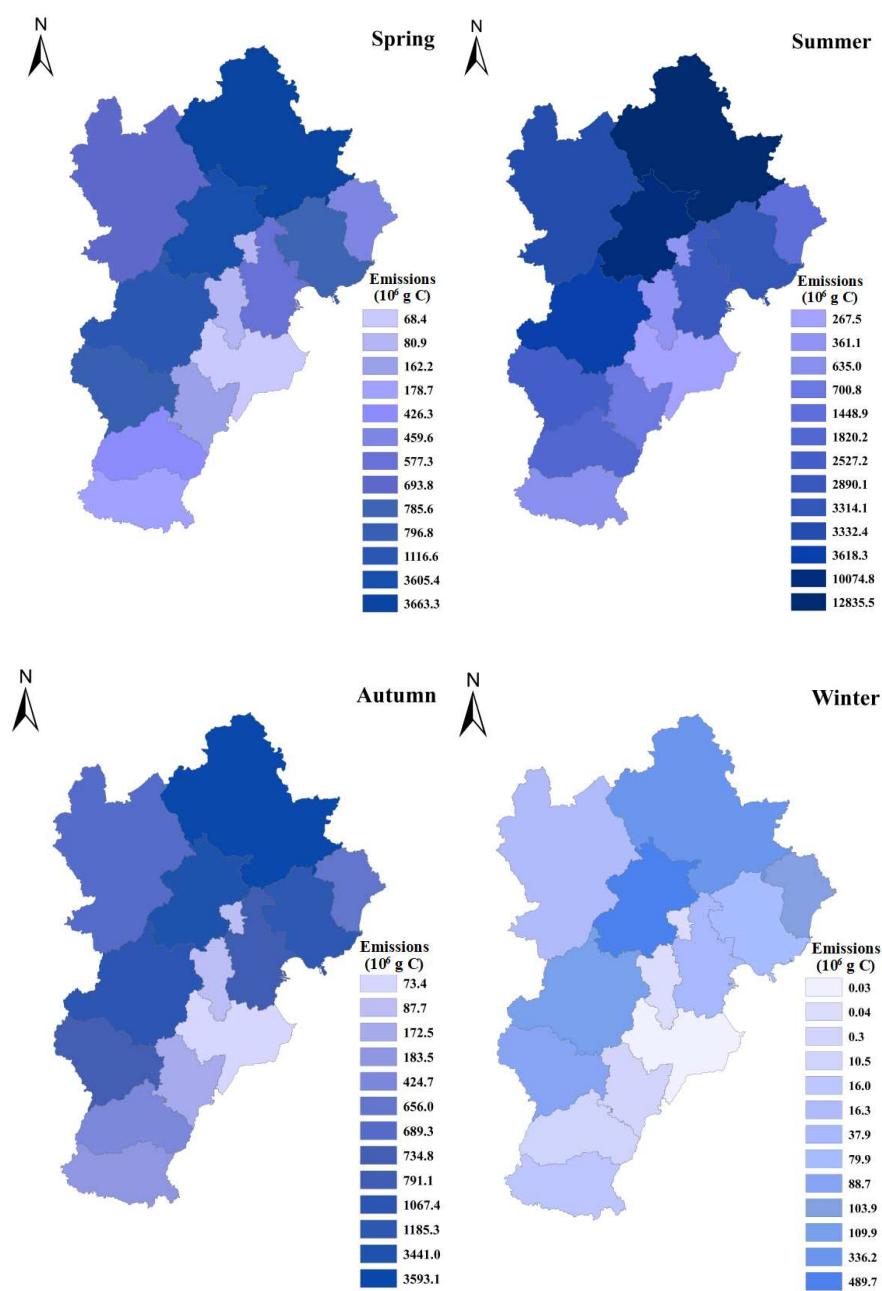


Figure 6. The seasonal BVOCs emissions distribution of dominant forest species in the Jing-Jin-Ji area (10^6 g C)

3.4 Chemical activity evaluation

The contribution of BVOCs to atmospheric chemical reaction depends on the level of its emissions and closely related to their chemical activity. Since the olefins with double bonds are more active ingredients compounds in addition with the main BVOCs components released by dominant forest species in the Jing-Jin-Ji area are isoprene and monoterpenes, the chemical activity of isoprene and monoterpenes by the maximum incremental reactivity (MIR) method and the $\cdot\text{OH}$ reaction rate (L^{OH}) method were comprehensively analyzed. **Figure 7** shows the OFP and L_i^{OH} values and activity contribution rates of every dominant forest species. Overall, the activity contribution rate of isoprene and monoterpenes of each species calculated using two methods is basically consistent. Among them, the OFP values of *Robinia pseudoacacia*, *Populus tomentosa* and *Quercus variabilis* obtained by the MIR method were higher, followed by *Betula platyphylla* and *Pinus tabulaeformis* while the lowest OFP values was obtained for *Ulmus pumila*. The forest species with higher L_i^{OH} value obtained by the L^{OH} method were *Robinia pseudoacacia*, *Populus tomentosa*, *Platycladus orientalis*, *Pinus tabulaeformis* and *Quercus variabilis* while *Larix gmelinii* had the lowest L_i^{OH} value. The difference between the two methods was due to their different principles in which the L^{OH} method reflects the reactivity by calculating the ability of BVOCs and OH radical to produce RO_2 without considering the influence of other subsequent reactions. Although the MIR method considers a series of responses of BVOCs, the lack of some MIR coefficients also affects the results. Based on the two approaches, *Robinia pseudoacacia*, *Populus tomentosa*, *Quercus variabilis* and *Pinus tabulaeformis* are the

dominant forest species that contribute higher BVOCs reaction activity in the Jing-Jin-Ji area. Among them, *Robinia pseudoacacia*, *Populus tomentosa* and *Quercus variabilis* have higher reactivity due to their higher isoprene activity contribution rate. The OFP and L^{OH} value of *Robinia pseudoacacia*, *Populus tomentosa*, *Quercus variabilis* were $156.76 \mu\text{g}/\text{m}^3$ and 138.36×10^5 , $87.19 \mu\text{g}/\text{m}^3$ and 78.86×10^5 , $87.19 \mu\text{g}/\text{m}^3$ and 78.86×10^5 , respectively. In addition, *Pinus tabulaeformis* was detected with higher activity contribution rate of monoterpenes, especially β -myrcene, limonene, and α -pinene, hence the OFP and L^{OH} were detected at $43.63 \mu\text{g}/\text{m}^3$ and 54.67×10^5 , respectively.

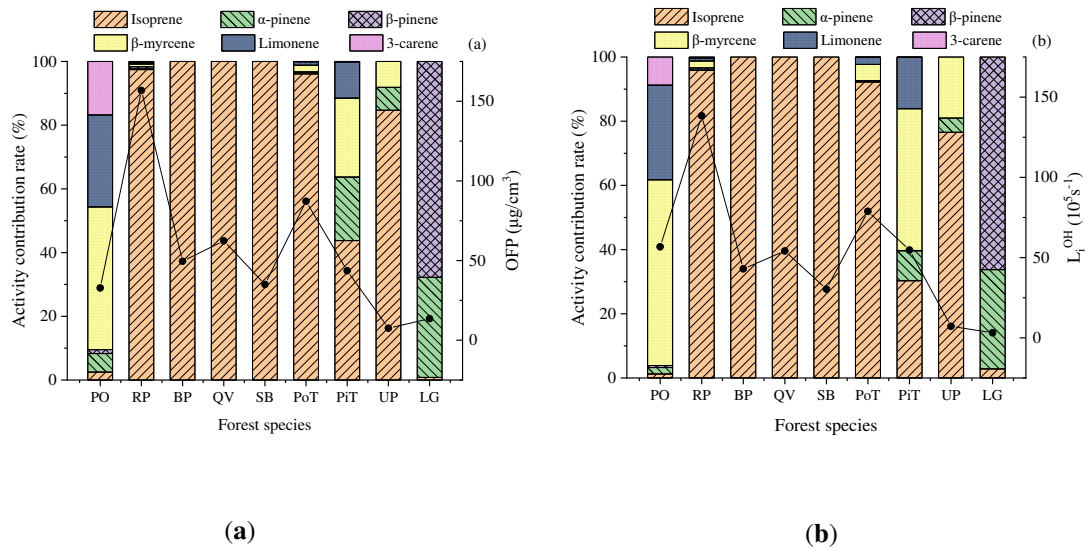


Figure 7. The reaction activity and activity contribution rate of BVOCs of dominant tree species in the Jing-Jin-Ji area calculated by MIR method (a) and L^{OH} method (b)

4. Uncertainty in BVOCs emission estimates

Since the emissions of BVOCs by vegetation are influenced by multiple factors, the uncertainty for the estimation needs to be taken into consideration. The primary sources of uncertainty in BVOCs emissions estimation include emission factors, leaf biomass, vegetation distribution, model algorithm and meteorological parameters. Estimation of total BVOCs emissions released by vegetation on the ground in the Jing-Jin-Ji area were studied using different algorithms and data sources. Different models, emission factors or vegetation type data would produce considerably different emissions (approximately doubling) (Carlton and Baker, 2011; Hogrefe et al., 2011; Chen et al., 2018). In view of the above, the BVOCs emissions estimated in our study are based on the field vegetation investigation and measured forest species emission rates as an effort to eliminate the uncertainties further. However, the emission rates obtained through experiments are mostly related to plant physiological conditions. Hence, the differences in the values could be due to uncertainty or uncontrollable stressors, environmental conditions, or genetically related metabolic processes (Loreto et al., 2009; Monson et al., 2013). For the sampling method, the dynamic headspace method used in this study has more air circulation than the static system, thus the real existing environment of plants can be maintained in good condition. However, the disturbance to plants during the process and the unrealistic high concentration of H₂O caused by transpiration may interfere with the leaf stomata; consequently the emissions could be impacted (Ortega et al., 2008). Moreover, the rapid reactivity of BVOCs would also affect the deviation of flux and the analysis performed by the GC-MS instrument may also possess potential

measurement errors. As for the emission factors in this study, the influence of solar radiation on monoterpene emissions is not considered in the calculation. The emission mechanism of different monoterpenes varies greatly in which some of the monoterpenes are reported to be positively correlated with temperature (Guenther et al., 2012). The harvesting of leaf biomass was calculated via the biological parameters such as forest vegetation accumulation and trunk density. It should be noted that the manual measurement errors would also affect the accuracy of the calculation. Furthermore, the meteorological data used in this study was retrieved from the MODIS satellite published on the NASA website. The acquisition, processing, analysis and conversion of satellite data would further introduce various types and degrees of uncertainty; thus there are differences between the satellite data and the local actual observation data such as solar radiation and air temperature. Overall, it is suggested that the future work should be emphasized on reduction and prevention of those uncertainties to obtain more accurate data.

5. Conclusions

The total annual emissions of BVOCs released from dominant forest species in the Jing-Jin-Ji area were estimated to be $70.8 \text{ Gg C}\cdot\text{a}^{-1}$. Isoprene, monoterpenes, and other VOCs contributed 40.5%, 36.0%, and 23.4%, respectively. As for monthly and seasonal variations, the emissions of BVOCs were peaked in summer (June, July, and August)

and bottomed out in winter (December, January, and February). This explains the summer represents the season with the most severe ozone pollution. In terms of spatial distribution, high BVOCs emissions were mainly distributed in the Taihang Mountains and the Yanshan Mountains. Chengde contributed the most followed by Beijing, inferring that these two cities should have more attention to mitigate BVOCs emissions to atmospheric ozone and particulate pollution. In terms of forest species, *Platycladus orientalis*, *Quercus variabilis*, *Populus tomentosa*, *Pinus tabulaeformis* and *Robinia pseudoacacia* are the primary contributors of BVOCs emissions and atmospheric reactivity. In conclusion, it is recommended that the use of these forest species for greening configuration should be avoided since they negatively impact the atmosphere due to high emissions or reactivity of BVOCs.

Abbreviations

BVOCs: Biogenic volatile organic compounds; AVOCs: Anthropogenic volatile organic compounds; G93: Guenther model developed in 1993; NMVOCs: non-methane volatile organic compounds; PANs: peroxyacetyl nitrate; SOA: secondary organic aerosols; PM: particulate matter; $\cdot\text{OH}$: Hydroxyl radical; PFT: plant functional types; PAR: photosynthetically active radiation; MIR: maximum incremental reactivity; L^{OH} : $\cdot\text{OH}$ reaction rate; OFP: Ozone formation potential; OVOCs: other VOCs; TVOCs: total VOCs; NIST: National Institute of Standards and Technology; PAMS: Photochemical

Assessment Monitoring Stations

Acknowledgements

Not applicable.

Authors' contributions

Xiaoxiu Lun and Ying Lin conceived the study; Ying Lin participated in study design, field measurements, data processing and writing the manuscript; Xiaoxi Jing and Chong Fan took part in the field measurements; Wei Tang and Zhongzhi Zhang took part in the procedure of data processing. All authors contributed critically to successive drafts and gave final approval for publication.

Funding

This work was supported by the grants from Beijing Municipal Science and Technology Project (No. Z181100005318003), National Research Program for Key Issues in Air Pollution Control (DQGG0201 and DQGG0107), National Natural Science Foundation of China (No. 41605077).

Availability of data and materials

The datasets used and/or analysed during the current study are available from the corresponding author on reasonable requests.

Ethics approval and consent to participate

Not applicable.

Consent for publication

Not applicable.

Competing interests

The authors declare that they have no competing interests.

References

Atkinson R, Arey J (2003) Atmospheric degradation of volatile organic compounds. *Chem. Rev.* 103 (12), 4605-4638.

<https://doi.org/10.1002/chin.200410285>.

Aksoyoglu S, Keller J, Barmpadimos I, Oderbolz D, Lanz VA, Prevot ASH (2011) Aerosol modelling in Europe with a focus on Switzerland during summer and winter episodes. *Atmos Chem Phys.* 11(14), 7355-7373.

<https://doi.org/10.5194/acp-11-7355-2011>.

Carlo P, Brune W, Martinez M, Harder H, Leshner R, Ren X, Thornberry T, Carroll M, Young V, Shepson P (2004) Missing OH reactivity in a forest: evidence for unknown reactive biogenic VOCs. *Science.* 304, 722-725.

<https://doi.org/10.1126/science.1094392>, 2004.

Carlton AG, Baker KR (2011) Photochemical modeling of the ozark isoprene volcano: MEGAN, BEIS, and their impacts on air quality predictions. *Environ. Sci.*

Technol. 45(10), 4438-4445.

<https://doi.org/10.1021/es200050x>.

Chen P, Quan J, Zhang Q, Tie X, Gao Y, Li X, Huang M (2013) Measurements of vertical and horizontal distributions of ozone over Beijing from 2007 to 2010. *Atmos. Environ.* 74, 37-44.

<https://doi.org/10.1016/j.atmosenv.2013.03.026>.

Chen WH, Guenther AB, Wang XM, Chen YH, Gu DS, Chang M (2018) Regional to global biogenic isoprene emission responses to changes in vegetation from 2000 to 2015. *J. Geophys. Res.-Atmos.* 123(7), 3757-3771.

<https://doi.org/10.1002/2017JD027934>.

Claeys M, Wang W, Ion AC, Kourtchev I, Gelencser A, Maenhaut W (2004) Formation of secondary organic aerosols from isoprene and its gas phase oxidation products through reaction with hydrogen peroxide. *Atmos. Environ.* 38(25), 4093-4098.

<https://doi.org/10.1016/j.atmosenv.2004.06.001>.

Carter, W (1991) Development of ozone reactivity scales for volatile organic compounds. *J. Air Waste Manage. Assoc.* 44, 881-899.

<https://doi.org/10.1080/1073161X.1994.10467290>.

Carter W (2008) Reactivity estimates for selected consumer product compounds. California: Center for environmental research and technology. College of engineering,

University of California.

Fehsenfeld F, Calvert J, Fall R, Goldan P, Guenther AB, Hewitt CN (1992) Emissions of volatile organic compounds from vegetation and the implications for atmospheric chemistry. *Glob. Biogeochem. Cycle.* 6 (4), 389-430.

<https://doi.org/10.1029/92GB02125>.

Filella I, Primante C, Llusà J, Martín González AM, Seco R, Farré-Armengol G (2013) Floral advertisement scent in a changing plant pollinators market. *Sci Rep.* 3(1), 3434.

<https://doi.org/10.1038/srep03434>.

Fan Chong (2019) Study on biogenic volatile organic compounds emission from forest plants in Hebei province. Beijing Forestry University. (in Chinese)

Ghirardo A, Xie J, Zheng X, Wang Y, Grote R, Block K (2016) Urban stress-induced biogenic VOC emissions and SOA-forming potentials in Beijing. *Atmos. Chem. Phys.* 16(5), 2901-2920.

<https://doi.org/10.5194/acp-16-2901-2016>.

Geng F, Tie X, Guenther A, Li G, Cao J, Harley P (2011) Effect of isoprene emissions from major forests on ozone formation in the city of Shanghai, China. *Atmos. Chem. Phys.* 11, 10449-10459.

<https://doi.org/10.5194/acp-11-10449-2011>.

Guenther A, Hewitt CN, Erickson D, Fall R, Geron C, Graedel T (1995) A global model of natural volatile organic compound emissions. *Atmos. Chem. Phys.* 100 (D5), 8873-8892.

<https://doi.org/10.1029/94JD02950>.

Guenther AB, Jiang X, Heald CL, Sakulyanontvittaya T, Duhl T, Emmons LK, Wang X (2012) The model of emissions of gases and aerosols from nature version 2.1 (MEGAN2.1) : an extended and updated framework for modeling biogenic emissions. *Geosci. Model Dev.* 5 (2), 1503-1560.

<https://doi.org/10.5194/gmdd-5-1503-2012>.

Guenther AB, Zimmerman PR, Harley PC, Monson RK, Fall R (1993) Isoprene and monoterpene emission rate variability: model evaluations and sensitivity analyses. *J. Geophys. Res.* 98 (D7), 12609-12617.

<https://doi.org/10.1029/93JD00527>.

Goldan P, Kuste W, Williams E, Murphy P (2004) Nonmethane hydrocarbon and oxy hydrocarbon measurements during the 2002 New England air quality study. *J. Geophys. Res.-Atmos.* 109 (21).

<https://doi.org/10.1029/2003JD004455>.

Hsu CY, Ching HC, Chen MJ, Chuang CY, Tsen CM, Fang GC, Tsai YI, Chen NT, Lin TY (2017) Ambient PM_{2.5} in the residential area near industrial complexes:

Spatiotemporal variation, source apportionment, and health impact. *Sci. Total Environ.* 590, 204-214.

<https://doi.org/10.1016/j.scitotenv.2017.02.212>.

Han X, Zhang M, Tao J, Wang L, Gao J, Wang S, Chai F (2013) Modeling aerosol impacts on atmospheric visibility in Beijing with RAMS-CMAQ. *Atmos. Environ.* 72, 177-191.

<https://doi.org/10.1016/j.atmosenv.2013.02.030>.

Hogrefe C, Isukapalli S, Tang X, Georgopoulos PG, He S, Zalewsky EE (2011) Impact of biogenic emission uncertainties on the simulated response of ozone and fine particulate matter to anthropogenic emission reductions. *J. Air Waste Manage. Assoc.* 61(1), 92-108.

<https://doi.org/10.3155/1047-3289.61.1.92>.

Klinger LF, Li QJ, Guenther AB, Greenberg JP, Baker B, Bai JH (2002) Assessment of volatile organic compound emissions from ecosystems of China. *J. Geophys. Res.* 107(D21), 4603.

<https://doi.org/10.1029/2001JD001076>.

Kulmala M, Nieminen T, Chellapermal R, Makkonen R, Bäck J, Kerminen VM (2013) Climate feedback linking the increasing atmospheric CO₂ concentration, BVOC emissions, aerosols and clouds in forest ecosystems. *Biology, Controls and Models of*

Tree Volatile Organic Compound Emissions. 489-508.

https://doi.org/10.1007/978-94-007-6606-8_17.

Laothawornkitkul J, Taylor JE, Paul N, Hewitt CN (2009) Biogenic volatile organic compounds in the Earth system. *New Phytol.* 183(1), 27-51.

<https://doi.org/10.1111/j.1469-8137.2009.02859.x>.

Li Z, Gu X, Wang L, Li D, Xie Y, Li K, Dubovik O, Schuster G, Goloub P, Zhang Y (2013) Aerosol physical and chemical properties retrieved from ground-based remote sensing measurements during heavy haze days in Beijing Winter. *Atmos. Chem. Phys.* 13(20), 10171-10183.

<https://doi.org/10.5194/acp-13-10171-2013>.

Li M, Ren X, Yu Y, Zhou L (2016) Temporal and spatial distribution of PM_{2.5} pollution in Chinese cities. *China Environmental Science.* 36(3), 641-650.

Li J, Li L, Wu R, Li Y, Bo Y, Xie S (2016) Inventory of highly resolved temporal and spatial volatile organic compounds emission in China. *Air Pollution.* 207(8), 79-86.

<https://doi.org/10.2495/AIR160081>.

Loreto F, Bagnoli F, Fineschi S (2009) One species, many terpenes: matching chemical and biological diversity. *Trends Plant Sci.* 14(8), 416-420.

<https://doi.org/10.1016/j.tplants.2009.06.003>.

Loreto F, Schnitzler JP (2010) Abiotic stresses and induced BVOCs. *Trends Plant Sci.* 15 (3), 154-166.

<https://doi.org/10.1016/j.tplants.2009.12.006>.

Meng X, Gong Z, Ye C, Wang S, Sun H, Zhang X (2016) Characteristics of ozone concentration variation in 74 cities from 2013 to 2016. *Environmental Monitoring in China.* 33(05),101-108.

<https://doi.org/10.19316/j.issn.1002-6002.2017.05.15>.

Monson RK, Jones RT, Rosenstiel TN, Schnitzler JP (2013) Why only some plants emit isoprene. *Plant Cell Environ.* 36(3), 503-516.

<https://doi.org/10.1016/10.1111/pce.12015>.

Ortega J, Helmig D, Daly R, Tanner DM, Guenther AB., Herrick JD (2008) Approaches for quantifying reactive and low-volatility biogenic organic compound emissions by vegetation enclosure techniques-part B: applications. *Chemosphere.* 72(3), 365-380.

<https://doi.org/10.1016/j.chemosphere.2008.02.054>.

Ran L, Zhao C, Xu W, Lu X, Han M, Lin W (2011) VOC reactivity and its effect on ozone production during the HaChi summer campaign. *Atmos. Chem. Phys.* 11(10), 4657-4667.

<https://doi.org/10.5194/acp-11-4657-2011>.

Steinbrecher R, Smiatek G, Koble R, Seufert G, Theloke J, Hauff K, Ciccioli P, Vautard R, Curci G (2009) Intra- and inter-annual variability of VOC emissions from natural and semi-natural vegetation in Europe and neighbouring countries. *Atmos. Environ.* 43(7), 1380-1391.

<https://doi.org/10.1016/j.atmosenv.2008.09.072>.

Sartelet KN, Couvidat F, Seigneur C, Roustan Y (2012) Impact of biogenic emissions on air quality over Europe and North America. *Atmos. Environ.* 53, 131-141.

<https://doi.org/10.1016/j.atmosenv.2011.10.046>.

Sicard P, Anav A, De Marco A, Paoletti E (2017) Projected global tropospheric ozone impacts on vegetation under different emission and climate scenarios. *Atmos. Chem. Phys.* 1-34.

<https://doi.org/10.5194/acp-2017-74>.

Song Y, Zhang Y, Wang Q, An J (2012) Estimation of biogenic VOCs emissions in Eastern China based on remote sensing data. *Acta Sci. Circumst.* 32(9), 2216-2227. (in Chinese).

Tang G, Li X, Wang Y, Xin J, Ren X (2009) Surface ozone trend details and interpretations in Beijing, 2001-2006. *Atmos. Chem. Phys.* 9 (22), 8813-8823.

<https://doi.org/10.5194/acp-9-8813-2009>.

Wang T, Xue L, Peter B, Yun F, Li L, Zhang L (2017) Ozone pollution in China: a

review of concentrations, meteorological influences, chemical precursors, and effects. *Sci. Total Environ.* 575, 1582-1596.

<https://doi.org/10.1016/j.scitotenv.2016.10.081>.

Wang L, Xu J, Yang J, Zhao X, Wei W, Cheng D (2012) Understanding haze pollution over the southern Hebei area of China using the CMAQ model. *Atmos. Environ.* 56, 69-79.

<https://doi.org/10.1016/j.atmosenv.2012.04.013>.

Wang X, Feng Z, Ouyang Z (2001) The impact of human disturbance on vegetative carbon storage in forest ecosystems in China. *For. Ecol. Manage.* 148(1-3), 117-123.

[https://doi.org/10.1016/S0378-1127\(00\)00482-5](https://doi.org/10.1016/S0378-1127(00)00482-5).

Xie X, Shao M, Liu Y, Lu S, Chang C, Chen Z (2008) Estimate of initial isoprene contribution to ozone formation potential in Beijing, China. *Atmos. Environ.* 42(24), 6000-6010.

<https://doi.org/10.1016/j.atmosenv.2008.03.035>.

Xia C, Xiao L (2019) Estimation of biogenic volatile organic compounds emissions in Jing-Jin-Ji. *Acta Sci. Circumst.* 39(8), 2680-2689. (in Chinese).

Zhao H, Zheng Y, Zhang Y (2020) Spatiotemporal distribution and population exposure of air pollution in Beijing-Tianjin-Hebei region. *Acta Sci. Circumst.* 40 (1), 1-12. (in Chinese).

Zhao P, Dong F, He D, Zhao X, Zhang X, Zhang W (2013) Characteristics of concentrations and chemical compositions for PM_{2.5} in the region of Beijing, Tianjin, and Hebei, China. *Atmos. Chem. Phys.* 13 (9), 4631-4644.

<https://doi.org/10.5194/acp-13-4631-2013>.

Zhai S, An X, Zhao T, Sun Z, Wang W (2016) Detecting critical PM_{2.5} emission sources and their contributions to a heavy haze episode in Beijing, China by using an adjoint mode. *Atmos. Chem. Phys.* 1-20.

<https://doi.org/10.5194/acp-2016-911>.

Zhang Q, Li H, He M, Lv L, Yang J (2018) Estimation of volatile organic compounds emission from frequently-used greening tree species in Tianjin City. *Research of Environmental Sciences.* 31(2), 245-253. (in Chinese).

Figures

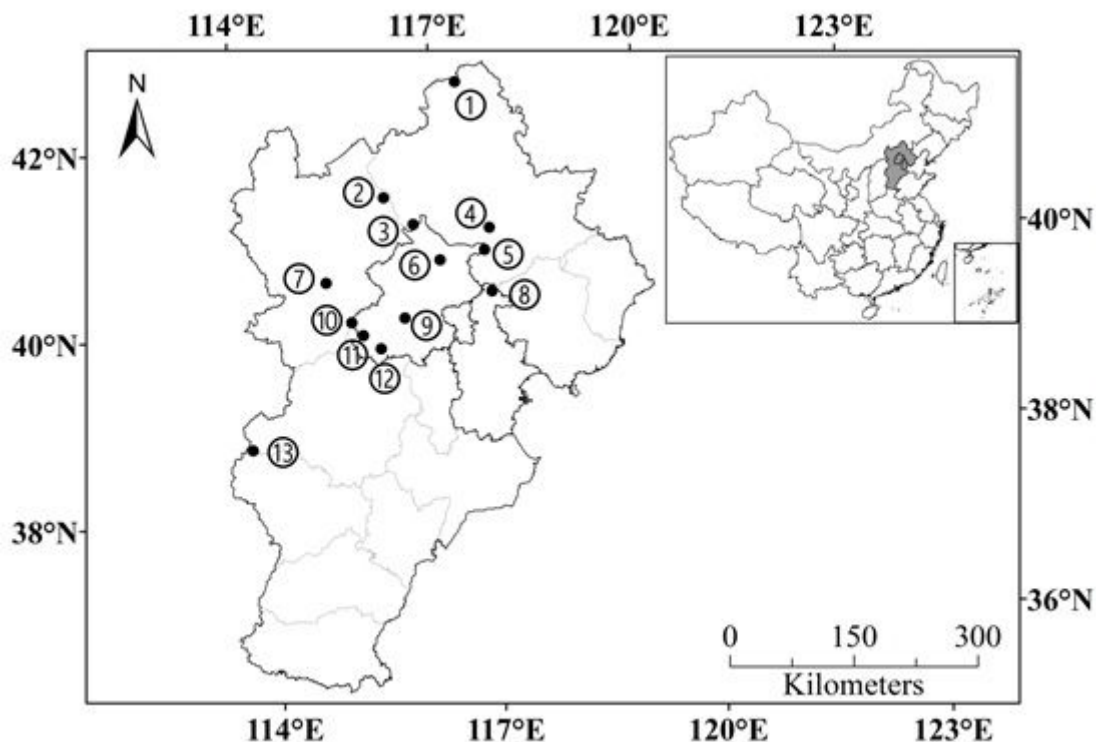


Figure 1

The site locations of the Jing-Jin-Ji area. The sampling sites (solid circles) identified as follows:
① Saihanba National Forest Park ② Heilongshan National Forest Park ③ Labagou Primeval Forest Park
④ Baicaowa National Forest Park ⑤ Wuling Mountain Scenic Spot ⑥ Yunmengshan National Forest Park
⑦ Huangyangshan Forest Park ⑧ Tianjin Jiulongshan National Forest Park ⑨ Xishan National Forest
Park ⑩ Xiaolongmen National Forest Park ⑪ Baihuashan National Nature Reserve ⑫ Shangfangshan
National Forest Park ⑬ Wuyuezhai Scenic Spot

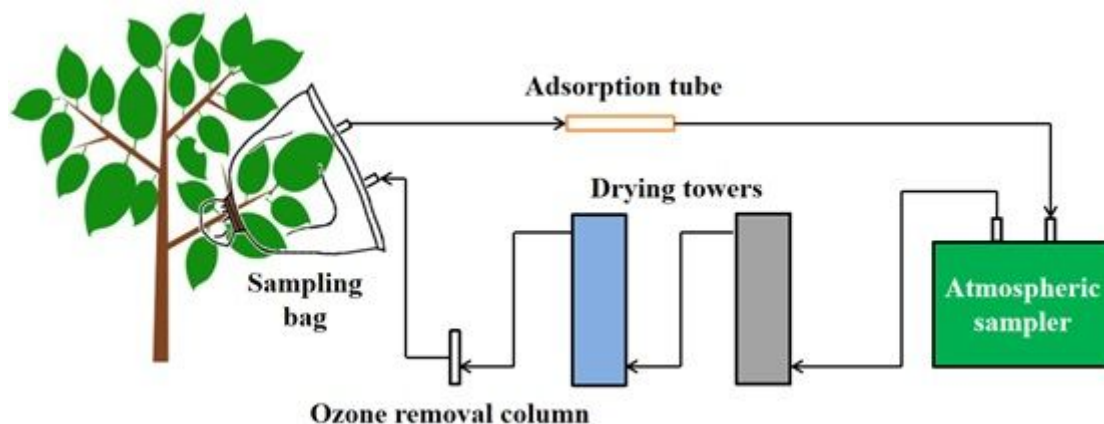


Figure 2

Flow chart of dynamic headspace sampling

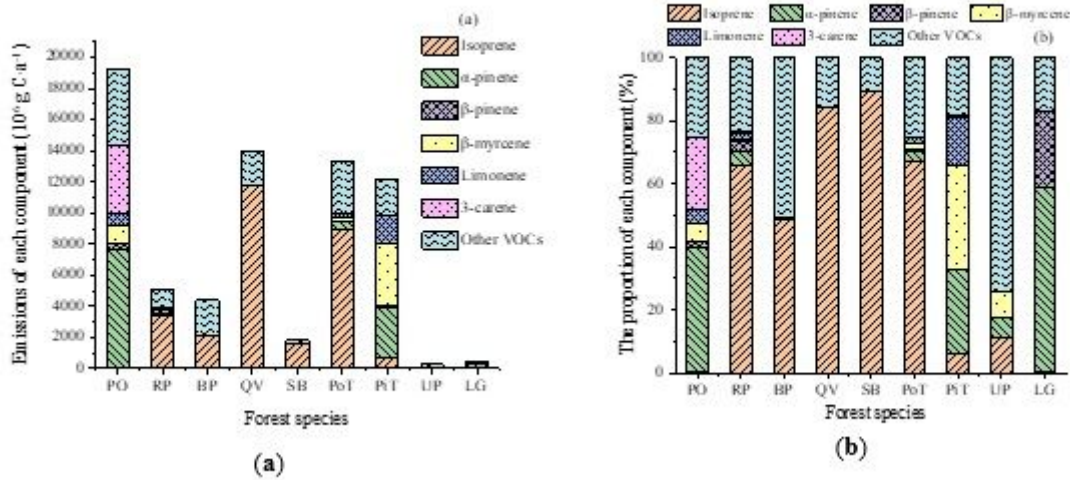


Figure 3

The BVOCs emissions (106 g C a^{-1}) (a) and proportion of each component (%) (b) from dominant forest species in the Jing-Jin-Ji area (BP: *Betula platyphylla*; QV: *Quercus variabilis*; UP: *Ulmus pumila*; PoT: *Populus tomentosa*; RP: *Robinia pseudoacacia*; PO: *Platycladus orientalis*; PiT: *Pinus tabuliformis*; SB: *Salix babylonica*; LG: *Larix gmelinii*)

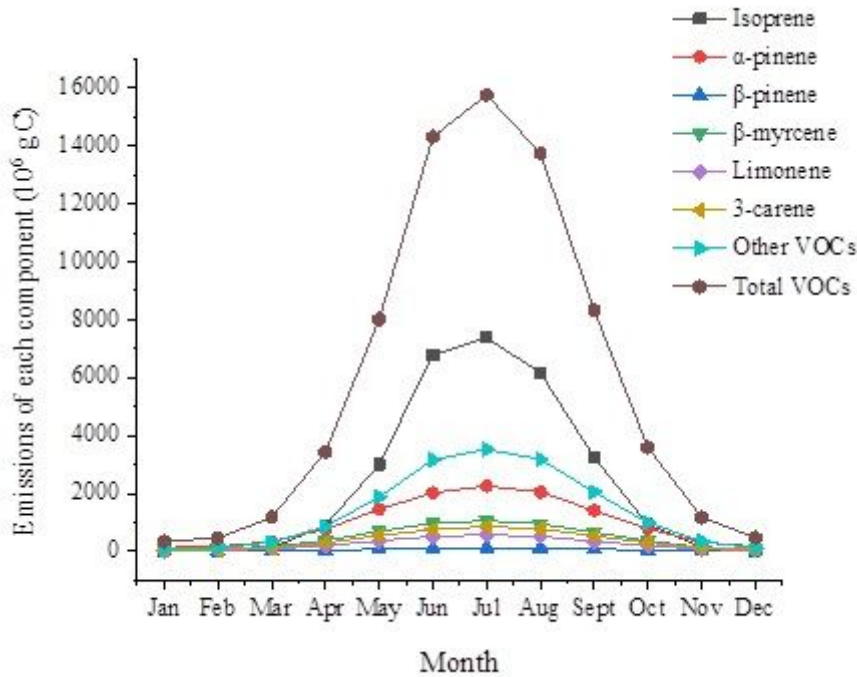


Figure 4

The monthly BVOCs emissions from dominant forest species in the Jing-Jin-Ji area (106 g C)

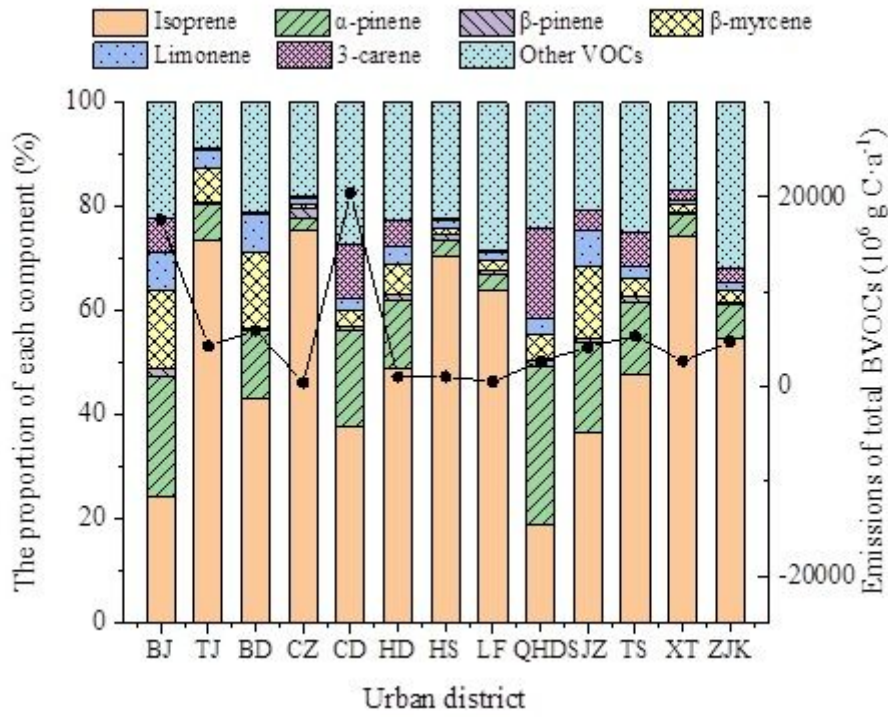


Figure 5

The BVOCs emissions ($10^6 \text{ g C}\cdot\text{a}^{-1}$) (a) and proportion of each component (%) (b) in each city in the Jing-Jin-Ji area (BJ: Beijing; TJ: Tianjin; BD: Baoding; CZ: Cangzhou; CD: Chengde; HD: Handan; HS: Hengshui; LF: Langfang; QHD: Qinhuangdao; SJZ: Shijiazhuang; TS: Tangshan; XT: Xingtai; ZJK: Zhangjiakou)

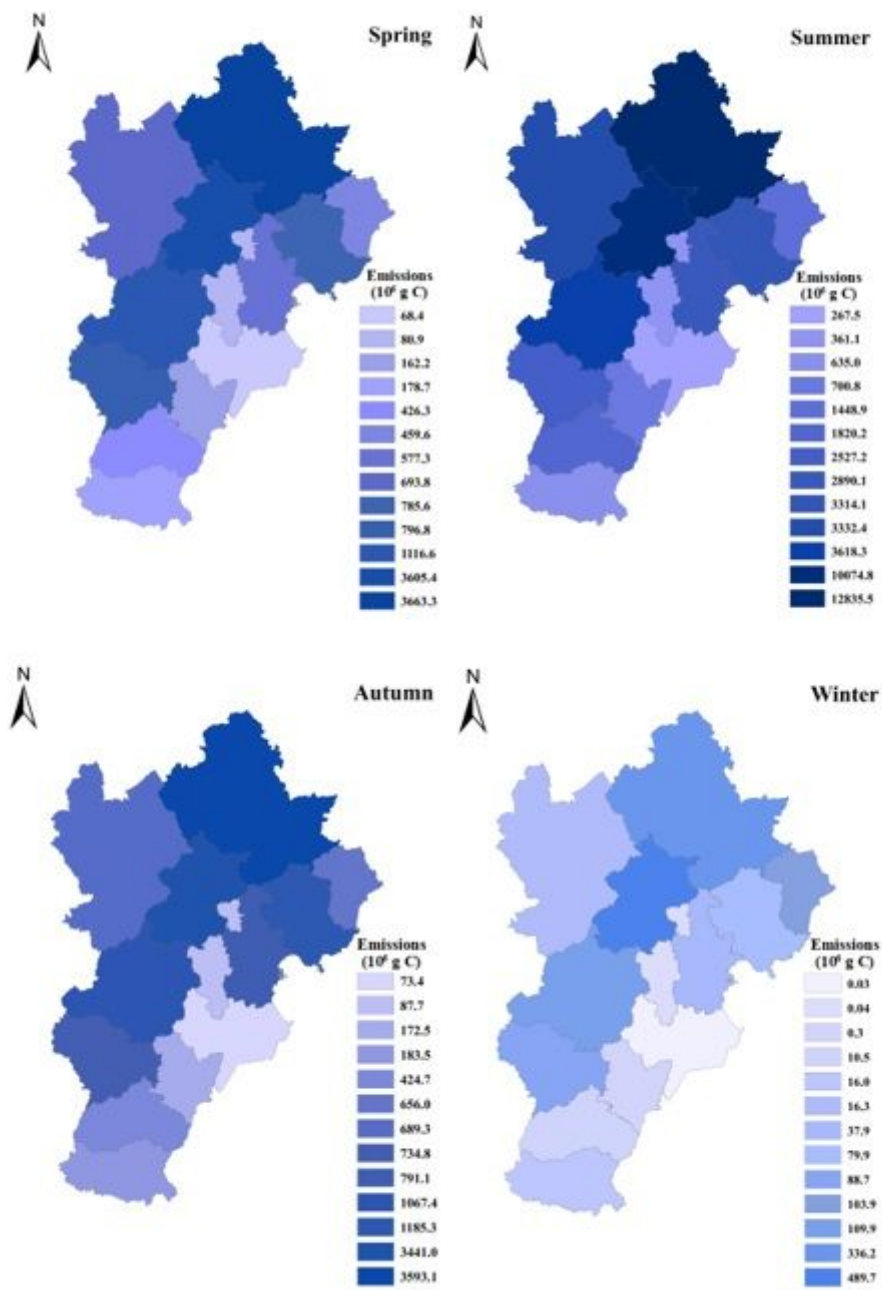


Figure 6

The seasonal BVOCs emissions distribution of dominant forest species in the Jing-Jin-Ji area (10^6 g C)

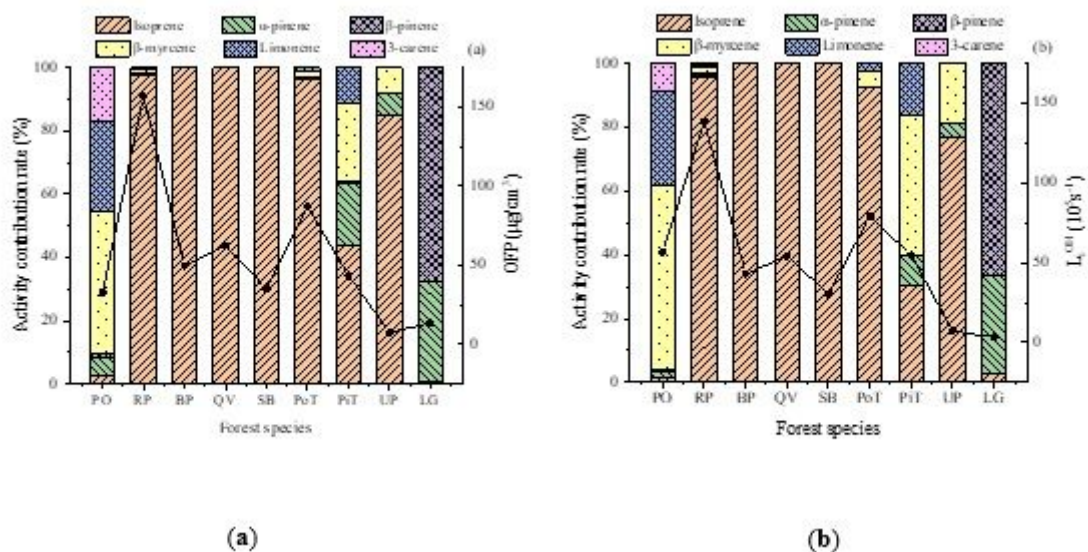


Figure 7

The reaction activity and activity contribution rate of BVOCs of dominant tree species in the Jing-Jin-Ji area calculated by MIR method (a) and LOH method (b)

Supplementary Files

This is a list of supplementary files associated with this preprint. Click to download.

- [Supplementarymaterialrevised.pdf](#)